

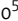



BRIEF DEFINITIVE REPORT

Interstitial-resident memory CD8⁺ T cells sustain frontline epithelial memory in the lung

Shiki Takamura¹, Shigeki Kato¹, Chihiro Motozono², Takeshi Shimaoka³, Satoshi Ueha³, Kazuhiko Matsuo⁴, Kosuke Miyauchi⁵, Tomoko Masumoto¹, Asami Katsushima¹, Takashi Nakayama⁴, Michio Tomura⁶, Kouji Matsushima³, Masato Kubo^{5,7}, and Masaaki Miyazawa^{1,8}

Populations of CD8⁺ lung-resident memory T (T_{RM}) cells persist in the interstitium and epithelium (airways) following recovery from respiratory virus infections. While it is clear that CD8⁺ T_{RM} cells in the airways are dynamically maintained via the continuous recruitment of new cells, there is a vigorous debate about whether tissue-circulating effector memory T (T_{EM}) cells are the source of these newly recruited cells. Here we definitively demonstrate that CD8⁺ T_{RM} cells in the lung airways are not derived from T_{EM} cells in the circulation, but are seeded continuously by T_{RM} cells from the lung interstitium. This process is driven by CXCR6 that is expressed uniquely on T_{RM} cells but not T_{EM} cells. We further demonstrate that the lung interstitium CD8⁺ T_{RM} cell population is also maintained independently of T_{EM} cells via a homeostatic proliferation mechanism. Taken together, these data show that lung memory CD8⁺ T_{RM} cells in the lung interstitium and airways are compartmentally separated from T_{EM} cells and clarify the mechanisms underlying their maintenance.

Introduction

Following resolution of infection, a subset of memory CD8⁺ T cells are established at the site of infection. These cells typically localized in the epithelial layer of the barrier tissues and are maintained independently of memory in the circulation, so called tissue-resident memory (T_{RM}) cells (Takamura, 2018). T_{RM} cells are primarily tissue memory CD8⁺ T cells and they play a key role in the immediate response to secondary infection. In contrast, CD8⁺ effector memory T (T_{EM}) cells (Sallusto et al., 1999; Masopust et al., 2001) or recently designated CX3CR1^{int} peripheral memory T cells that circulate between tissues and blood (Gerlach et al., 2016; Herndler-Brandstetter et al., 2018) are found to be a minority population in the peripheral tissues and exert a relatively small contribution to protection at the borders (Wu et al., 2014; Steinert et al., 2015). The later phases of the recall response are mediated by central memory T cells that survey secondary lymphoid organs and are activated in the draining lymph nodes. These cells undergo extensive proliferation to generate secondary effector cells, and provide protective immunity.

It is well known that CD8⁺ T_{RM} cells persist in the two distinct compartments of the lung: the interstitium and the epithelium (airways). Given the structural and functional differences

between these compartments, CD8⁺ T_{RM} cells in the lung airways and interstitium differ significantly in their phenotype, function, and maintenance. First, T_{RM} cells down-regulate the integrin LFA-1 (CD11a) once they enter the airway, thereby losing cell contact-mediated cytolytic potential (Hogan et al., 2001; Ely et al., 2006; Kohlmeier et al., 2007). However, they are able to provide heterosubtypic protection through the rapid and robust production of IFN- γ (McMaster et al., 2015). Second, airway CD8⁺ T_{RM} cells have a relatively limited lifespan due primarily to their biophysical removal, mediated by barrier function of the airway mucosa (Ely et al., 2006). Thus, it has been proposed that the population of airway CD8⁺ T_{RM} cells is dynamically maintained by the continual recruitment of CD8⁺ T_{EM} cells from the circulation (Ely et al., 2006; Zammit et al., 2006). A similar mechanism has been proposed for the maintenance of T_{RM} cells in the lung interstitium (Slütter et al., 2017). However, these proposed T_{EM} cell-dependent mechanisms of T_{RM} cell maintenance in the lung airways and interstitium are inconsistent with our recent findings regarding the circulatory memory-independent maintenance of lung T_{RM} cells (Takamura et al., 2016).

¹Department of Immunology, Kindai University Faculty of Medicine, Osaka, Japan; ²Department of Molecular Immunology, Research Institute for Microbial Diseases, Osaka University, Osaka, Japan; ³Division of Molecular Regulation of Inflammatory and Immune Diseases, Research Institute for Biomedical Sciences, Tokyo University of Science, Chiba, Japan; ⁴Division of Chemotherapy, Kindai University Faculty of Pharmacy, Osaka, Japan; ⁵Laboratory for Cytokine Regulation, Center for Integrative Medical Sciences, RIKEN Yokohama Institute, Kanagawa, Japan; ⁶Laboratory of Immunology, Faculty of Pharmacy, Osaka Otani University, Osaka, Japan; ⁷Division of Molecular Pathology, Research Institute for Biomedical Science, Tokyo University of Science, Chiba, Japan; ⁸Anti-Aging Center, Kindai University, Osaka, Japan.

Correspondence to Shiki Takamura: takamura@med.kindai.ac.jp.

© 2019 Takamura et al. This article is distributed under the terms of an Attribution–Noncommercial–Share Alike–No Mirror Sites license for the first six months after the publication date (see <http://www.rupress.org/terms/>). After six months it is available under a Creative Commons License (Attribution–Noncommercial–Share Alike 4.0 International license, as described at <https://creativecommons.org/licenses/by-nc-sa/4.0/>).

To address this discrepancy, we have undertaken a detailed analysis of the maintenance of lung memory T cells. Here we provide conclusive evidence that T_{RM} cells in the lung airways are maintained via the continual recruitment of T_{RM} cells from the lung interstitium, and that circulating T_{EM} cells are not involved in this process. Furthermore, we demonstrate that this process is regulated by CXCR6 expressed uniquely on T_{RM} cells but not on T_{EM} cells. We also demonstrate that interstitial T_{RM} cells are maintained by a process of homeostatic proliferation. Taken together, these data show that lung memory $CD8^+ T_{RM}$ cells in the lung interstitium and airways are compartmentally separated from T_{EM} cells and resolve the current debate on the underlying mechanism of their maintenance.

Results and discussion

Lung airway $CD8^+ T_{RM}$ cells are not replaced by memory $CD8^+ T$ cells from the circulation under steady-state conditions

To precisely discriminate $CD8^+ T_{RM}$ cells from tissue-circulating $CD8^+ T_{EM}$ cells in the lung, we used a combination of parabiosis and i.v. staining. Congenically distinct, influenza-immune mice were surgically joined after memory had been established (Fig. 1 A). 2 wk later, a $CD8\beta$ antibody (Ab) was administered i.v. to stain cells in the circulation (so that they could be distinguished during subsequent analysis), and tissues were harvested immediately thereafter (Fig. 1 B). 2 wk of parabiosis resulted in natural healing-mediated vascular anastomosis, which led to equilibration of host- and partner-derived memory $CD8^+ T$ cells in the circulation (Fig. 1 C, spleen). In contrast, host cells expressing typical T_{RM} cell phenotypes ($CD69^+CD103^+CD49a^+$) predominated in the lung interstitium and airways (Fig. 1, B and C). A minor proportion of partner cells in the lung interstitium and airways (mostly $CD69^-CD103^-CD49a^-$) represented tissue-circulating $CD8^+ T_{EM}$ cells (Fig. 1 B).

Previous reports have suggested that continual recruitment of cells from the circulation is required for the maintenance of $CD8^+ T_{RM}$ cells in the airways (Ely et al., 2006) and the lung interstitium (Slütter et al., 2017). In both of these cases, the ratio of partner cells in the lung should increase over time. However, we observed no differences in the ratio of host and partner cells in the lung interstitium and airways at 6 wk after surgery (Fig. 1 C). This indicates that, as in other mucosal tissues, cells in the circulation (including tissue-circulating $CD8^+ T_{EM}$ cells) have little, if any, contribution in the maintenance of $CD8^+ T_{RM}$ cells in the lung. Nevertheless, we paradoxically observed residual expression of CD11a on $CD8^+ T$ cells in the lung airways (Fig. 1 D). Since CD11a is completely down-regulated within 48 h after T cells enter the lung airway, these $CD11a^+ CD8^+ T$ cells must represent newly recruited cells (Ely et al., 2006). These $CD11a^+ CD8^+ T$ cells in the airways were constantly detected at a slightly higher ratio in the partner (Fig. 1 E), indicating that, consistent with a previous report (Ely et al., 2006), there is a continual influx of cells to this tissue.

To further investigate whether memory $CD8^+ T$ cells in the airways are replenished by new immigrants, we intratracheally (i.t.) transferred CFSE-labeled $CD8^+ T$ cells into the airways to determine whether these cells would be diluted by the continual

influx of cells from other sites (Fig. 1 F). Note that cells in the lung airways do not return to the circulation or proliferate within this tissue (Hogan et al., 2002). 7 d after transfer, donor cells completely down-regulated CD11a expression with no emergence of CFSE^{lo} cells, indicating that cells adapted to this tissue without proliferation (Fig. 1, G and H). While the proportions of donor cells were stable in the naive recipients for at least 7 d after transfer, we observed a significant reduction in the proportion of donor $CD8^+ T$ cells in the airways of A/HKx31 (x31)-immune recipients (Fig. 1, I and J). The rate of decline in the proportion of donor $CD8^+ T$ cells was significantly higher in i.n.-infected recipients compared with i.p.-infected recipients (which have T_{EM} cells in the circulation, but no T_{RM} cells in the lung interstitium), indicating a stronger cell influx to the airways in the former (Fig. 1, I and J). As similar numbers of donor cells could be recovered from the airways irrespective of prior respiratory virus infection (Fig. 1 K), the progressive contraction of donor cell population is due to the continual influx of recipient cells in the x31-immune mice (Fig. 1 G, see $CD11a^{hi}$ cells). Note that i.t. delivery had essentially no impact on the continual influx of recipient memory $CD8^+ T$ cells to the airways as determined by CD11a expression on airway memory cells 1 d after transfer (Fig. 1 L). Taken together, these data indicate that although memory $CD8^+ T$ cells in the circulation do not contribute to the maintenance of $CD8^+ T_{RM}$ cells in the lung interstitium and airways, memory $CD8^+ T$ cells in the lung airways are a dynamic population that is continuously replenished by new cells from a noncirculatory source.

A $CD8^+ T_{RM}$ cell pool in the lung interstitium, but not memory in the circulation, mediates the continual recruitment of memory $CD8^+$ cells to the lung airways

Since T_{EM} cells are not the source of airway T_{RM} cells, we considered the possibility that the airways are continuously seeded by $CD8^+ T$ cells from the lung interstitium (mostly T_{RM} cells). If this is the case, the TCR repertoire of $CD8^+ T_{RM}$ cells in the lung airways should significantly overlap with that in the lung interstitium. To test this idea, nucleoprotein (NP)-specific memory $CD8^+ T$ cells in the spleen, lung interstitium, and airways (cells in the lung interstitium and airways were further gated on $CD69^+$ to enrich T_{RM} cells) were subjected to TCR β -chain sequencing. As shown in Fig. 2, A and B, a large proportion of clones detected in the lung airways of individual mice was identical to those detected in the lung interstitium (ranging from 35.4 to 90.4%). Notably, $CD8^+ T_{RM}$ cells in the lung interstitium and airways invariably shared the dominant clonotypes, strongly suggesting that T_{RM} cells in the lung interstitium are the source of airway memory (Fig. 2 A). In some animals, a majority of clones, including the dominant ones in the airways, were also detected in the spleen (Fig. 2, see type 1), supporting a previous finding that central and resident memory $CD8^+ T$ cells may be derived from a common naive T cell precursor (Gaide et al., 2015). Interestingly, despite highly overlapping TCR repertoires between the lung interstitium and airways, relatively few identical TCR clonotypes were detected between the spleen and lung airways of mice (categorized in a second typing and ranging from 2 to 25.6%). In this case, we observed a disparate

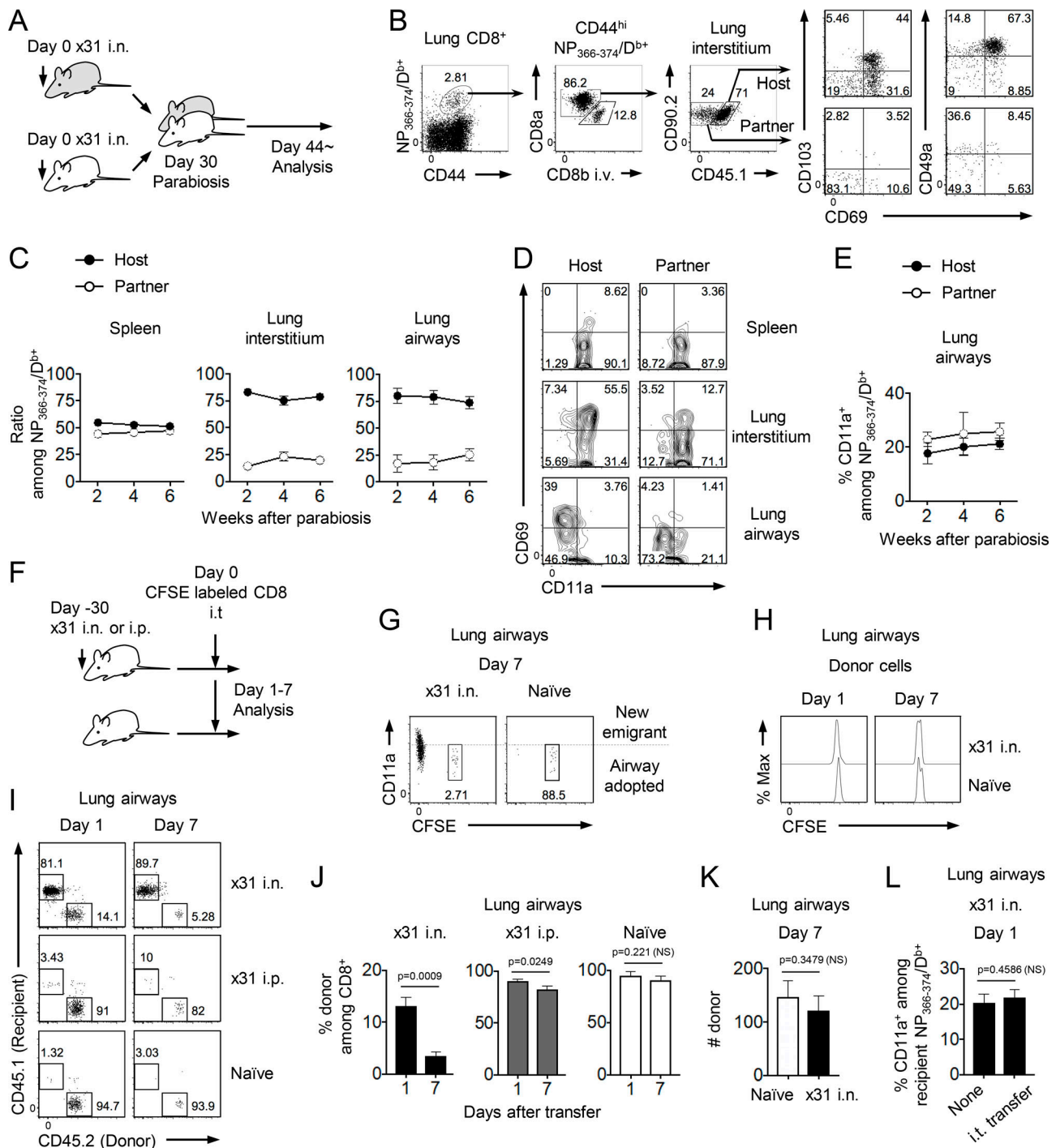


Figure 1. Lung airway memory CD8⁺ T cells are a unique type of T_{RM} cells in terms of their maintenance. (A) Experimental design for B–E. Congenic mice were infected i.n. with x31 and were subjected to parabiotic surgery 30 d later. (B) Gating protocol for host and partner NP-specific CD8⁺ T cells in the lung interstitium. The same gates were also used for lung airway cells. (C) Host/partner ratios of NP-specific CD8⁺ T cells in each tissue. (D) Expression of CD69 and CD11a on host and partner NP-specific CD8⁺ T cells in each tissue at day 14 after surgery. (E) Ratios of CD11a⁺ cells among host and partner NP-specific CD8⁺ T cells in the lung airways. (F) Experimental design for G–K. Total CD8⁺ T cells were isolated from the spleens of mice that had been previously infected with x31, then labeled with CFSE and transferred i.t. into congenically distinct x31-infected recipients at day 30 after infection. (G) Representative plots of recipient (CFSE-negative) and CFSE-labeled donor CD8⁺ T cells isolated from the lung airways of recipient mice at day 7 after transfer. (H) CFSE dilution of donor CD8⁺ T cells isolated from the lung airways of recipient mice at day 1 and 7 after transfer. (I) Representative plots of donor and recipient CD8⁺ T cells in the airways at day 1 and 7 after transfer. (J) Ratios of donor cells among total CD8⁺ T cells in the lung airway of recipient mice. (K) Numbers of donor cells isolated from the lung airways of recipient mice at day 7 after transfer. (L) Ratios of CD11a⁺ cells among recipient NP-specific CD8⁺ T cells in the lung airways 1 d after transfer. Data are representative of two independent experiments (mean and SD of three [F–L] to four [A–E] mice per group). Data were analyzed by unpaired t test (J–L). Error bars represent mean ± SD of three (F–L) or four (A–E) mice per group. Max, maximum.

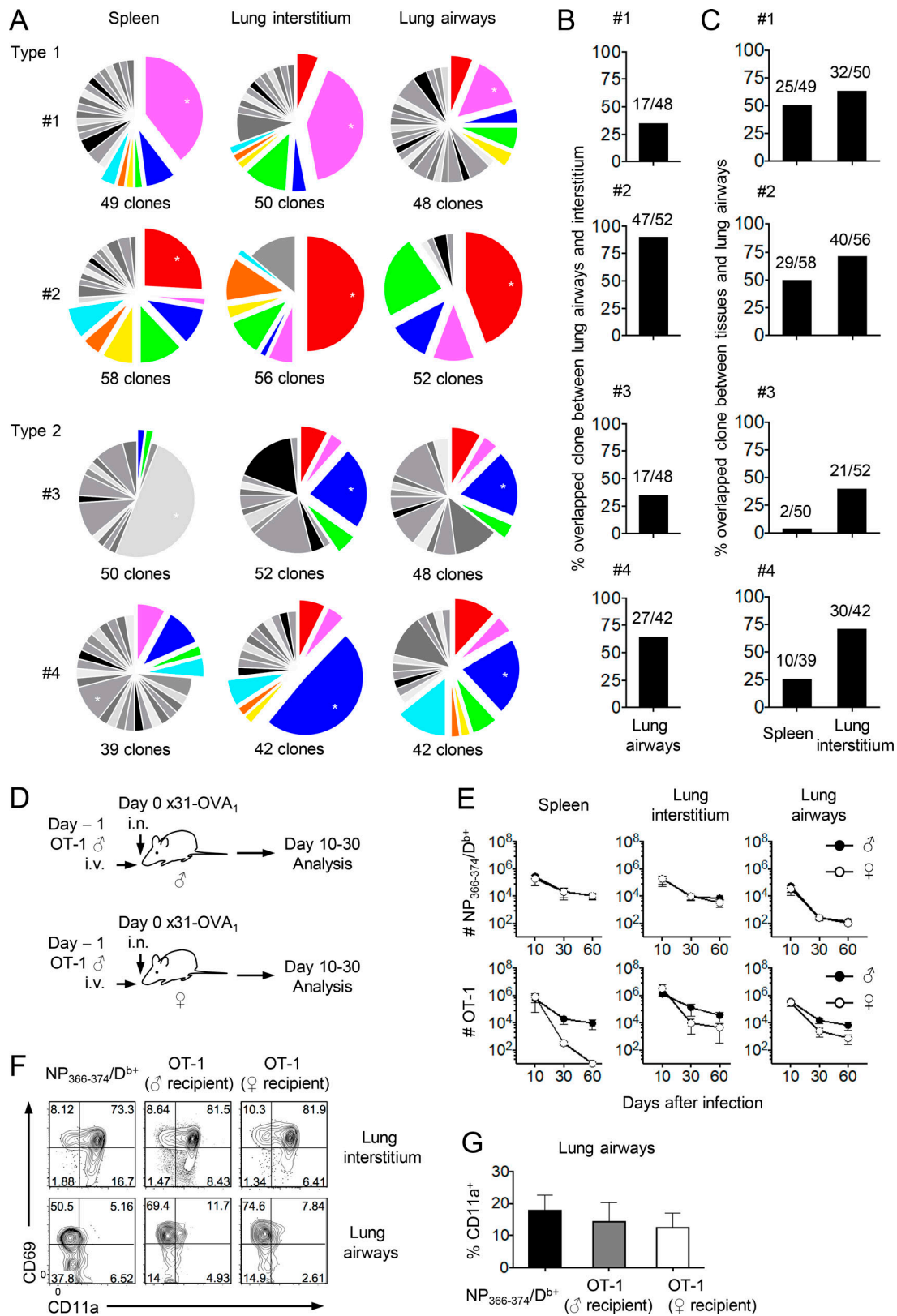


Figure 2. **CD8⁺ T_{RM} cells in the lung interstitium are a source of memory T_{RM} cells in the airways.** (A) The pie charts show the frequencies of different TCRβ clonotypes of NP-specific CD8⁺ T cells isolated from each tissue of mice on day 30 after x31 infection. Cells in the lung interstitium and airways were further gated on CD69⁺ to enrich T_{RM} cells. Identical clones found in the different tissues of individual animal were similarly colored (no relationship between distinct mice). Asterisks indicate dominant clones in each tissue. Numbers indicate total clones analyzed. (B) Percentage of identical clones between the lung interstitium and airways among those in the lung airways. The numbers indicate the number of identical clones over the total number of clones. (C) Percentage of identical clones with those in the lung airways in each tissue. The numbers indicate the number of identical clones over the total number of clones. Panels

A–C show representative data from four individual animals. **(D)** Experimental design for E–G. Naive CD8⁺ T cells isolated from male OT-1 mice (OT-1 cells) were transferred into congenically distinct male or female recipient mice, which were then infected i.n. with x31-OVA₁. **(E)** Numbers of NP-specific CD8⁺ T cells and OT-1 cells in each tissue at indicated time points. **(F)** Expression of CD69 and CD11a on NP-specific CD8⁺ T cells and OT-1 cells in the lung interstitium and airways at day 60 after infection. **(G)** Percentages of CD11a⁺ cells among NP-specific CD8⁺ T cells and OT-1 cells in the lung airways at day 60 after infection. Data are representative of two independent experiments (D–G; mean and SD of three [E] or six [G] mice per group). Error bars represent mean ± SD of three (E) or six (G) mice per group.

array of dominant clonotypes between the two tissues (Fig. 2, A and C, see type 2). These data support our hypothesis that the source of continual recruitment to the lung airways is a pool of CD8⁺ T_{RM} cells in the lung interstitium rather than the pool of memory CD8⁺ T cells in the circulation.

To further assess this issue, we asked whether CD8⁺ T_{RM} cells in the lung airways could be maintained in the absence of memory cells in the circulation. Male naive ovalbumin-specific CD8⁺ T cells (OT-1 cells) were transferred into either male or female recipient mice, which were then infected with recombinant influenza virus x31-OVA₁ (Fig. 2 D). In this model, a natural female anti-H-Y response leads to the depletion of male OT-1 cells, especially at the late phase of infection (Gebhardt et al., 2011; Slütter et al., 2017). Since CD8⁺ T_{RM} cells in tissues are significantly less susceptible to depletion compared with memory T cells in the circulation (Gebhardt et al., 2011; Schenkel et al., 2014; Takamura et al., 2016; Slütter et al., 2017), memory CD8⁺ T cells in the circulation should disappear faster than T_{RM} cells in the lung. As expected, male OT-1 cells were completely depleted in the spleen by day 60 after infection in the female recipient, whereas CD8⁺ T_{RM} cells in the lung interstitium and airways remained (Fig. 2 E). There were no differences in the NP-specific CD8 T cell responses between male and female recipients, indicating that depletion of splenic OT-1 cells has no impact on anti-flu cellular immunity (Fig. 2 E). Thus, the data clearly demonstrated that CD8⁺ T_{RM} cells in the lung airways are maintained in the absence of memory in the circulation. Even after OT-1 cells but not NP-specific memory CD8⁺ T cells were depleted from the circulation, we observed a similar frequency of CD11a expression on OT-1 and NP-tetramer⁺ cells in the lung airways (Fig. 2, F and G). This further supports our conclusion that CD8⁺ T_{RM} cells in the lung airways are maintained by continual recruitment from those in the lung interstitium.

Lung interstitium CD8⁺ T_{RM} cells undergo homeostatic proliferation independently of cells in the spleen

The numbers of CD8⁺ T_{RM} cells in the lung interstitium are stable for several months following recovery from a respiratory virus infection (Takamura et al., 2016), suggesting that proliferation of T_{RM} cells within the interstitium is required to compensate for the continuous loss of cells by intraepithelial migration. We first investigated whether there is local antigen-driven reactivation and proliferation of CD8⁺ T_{RM} cells in the lung interstitium. However, parabiosis of influenza-immune fluorescent ubiquitination-based cell cycle indicator (Fucci) transgenic (Tg) mice, which enables real-time visualizing cell cycle progression by tracking the expression of cell cycle-

specific proteins Cdt1 and Geminin (Sakaue-Sawano et al., 2008; Tomura et al., 2013), revealed that most reactivated (CD69⁺) CD8⁺ T_{RM} cells in the lung interstitium were quiescent (in the G₀ phase) with minimum evidence of ongoing proliferation (Fig. 3, A and B; see host).

An alternative possibility is that there is homeostatic proliferation of CD8⁺ T_{RM} cells in the lung that is independent of local reactivation. To test this idea, we administered the thymidine analogue BrdU in the drinking water following parabiotic surgery (Fig. 3 C). Host CD8⁺ T_{RM} cells in the lung interstitium incorporated BrdU, although to a lesser extent than memory CD8⁺ T cells in the circulation (all partner cell populations and host splenocytes; Fig. 3, D and E). Low-level BrdU incorporation was also evident in memory CD8⁺ T cells in the lung airways (Fig. 3, D and E), which is a nonproliferating population (Fig. 1 G). This suggests that airway memory cells incorporate BrdU before migration to that tissue. To test this idea, we administered BrdU at different time points and compared the frequencies of BrdU incorporation in different cell populations. As shown in Fig. 3, F and G, similar frequencies of BrdU⁺ cells were observed in the host populations of both the lung interstitium and the airways (although significantly lower than in circulatory memory cells). These data support the idea that airway memory cells originate from cells in the lung interstitium but not from the circulation (Fig. 3 E). Furthermore, BrdU incorporation was first evident in the interstitium but not in the airways, demonstrating the lung interstitium as a primary site of homeostatic proliferation of CD8⁺ T_{RM} cells (Fig. 3 G, see host, 1 h). Note that the lack of BrdU⁺ cells in the airways 1 h after BrdU administration was not simply due to limited diffusion of BrdU to this tissue, as airway cells incorporated CFSE in the same experimental setting (Fig. 3 G, see bottom panels). Phenotypic profiling revealed that BrdU incorporation was lowest in the bona fide CD8⁺ T_{RM} cell population (host CD69⁺CD103⁺) in the lung interstitium (Fig. 3 F). Higher BrdU incorporation by host CD69⁺CD103⁺ cells may indicate that this population is derived from host circulatory memory (Fig. 3 F). The lower turnover ratio of tissue memory suggests that there is limited availability of homeostatic cytokines in the T_{RM} cell niches in the lung interstitium as compared with the secondary lymphoid tissues. We also performed BrdU experiments using the depletion model (Fig. 3 G; see also Fig. 2 E). In this case, BrdU⁺CD8⁺ T_{RM} cells in the lung interstitium could be detected even when BrdU was administered after depletion of circulatory memory CD8⁺ T cells (Fig. 3 H). Together, the data conclusively demonstrate that lung interstitium CD8⁺ T_{RM} cells undergo homeostatic proliferation within this tissue and provide a source of cells to continuously seed cells to the airways.

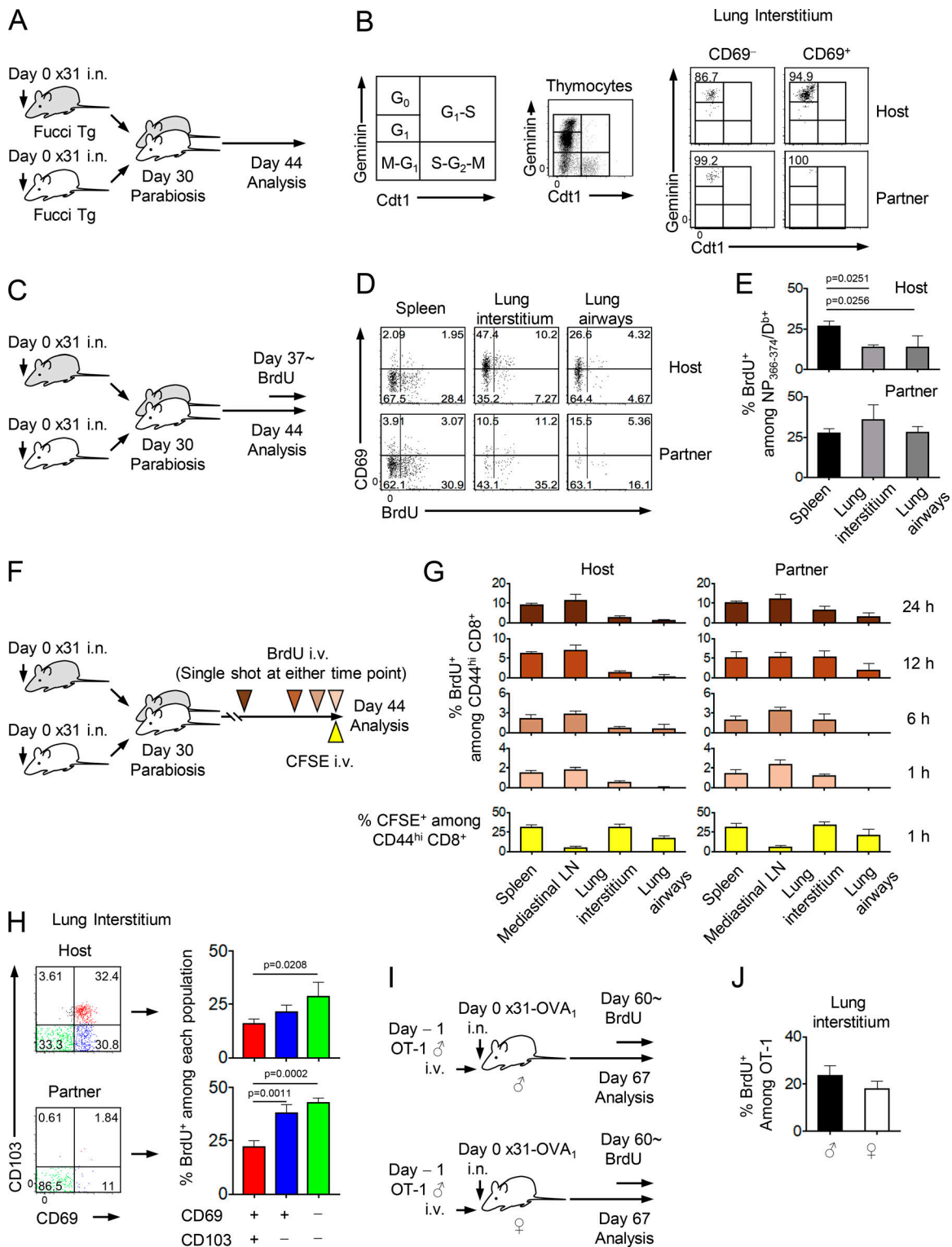


Figure 3. **Reactivation-independent self-renewal of CD8⁺ T_{RM} cells in the lung interstitium.** (A) Experimental design for B. Congenically distinct Fucci Tg mice were infected i.n. with x31 and then subjected to parabiotic surgery 30 d later. (B) Gating strategy for the analysis of cell cycle dynamics using Fucci Tg system. The central plot illustrates the gating strategy using thymocytes. The plots in the right illustrate the expression of Cdt1 and Geminin in host and partner NP-specific CD8⁺ T cells in the lung interstitium at day 14 after surgery. (C) Experimental design for D, E, and H. Congenic mice were infected i.n. with x31 and were subjected to parabiotic surgery 30 d later. BrdU was administered by drinking water from day 37 after infection (day 7 after surgery) for 1 wk. (D) Incorporation of BrdU in host and partner NP-specific CD8⁺ T cells in each tissue at day 14 after surgery. (E) Ratios of BrdU⁺ cells among host and partner NP-specific CD8⁺ T cells in each tissue at day 14 after surgery. (F) Experimental design for G. Parabiotic mice were administered i.n. with BrdU or CFSE at either time point before harvest. (G) Incorporation of BrdU or CFSE (bottom panels) in host and partner CD44^{hi} CD8⁺ T cells in each tissue of mice injected with BrdU or CFSE at indicated time points before harvest. (H) Incorporation of BrdU in indicated populations of host and partner NP-specific CD8⁺ T cells in the lung

interstitium. (I) Experimental design for J. Naive CD8⁺ T cells isolated from male OT-1 mice (OT-1 cells) were transferred into congenically distinct male or female recipient mice, which were then infected i.n. with x31-OVA. (J) Percentage of BrdU⁺ cells among OT-1 cells in the lung interstitium of recipient animals at day 67 after infection. Data are representative of two independent experiments (mean and SD of four mice per group). Error bars represent mean \pm SD of four (E, G, H, and J) mice per group. Data were analyzed by one-way ANOVA with Tukey's multiple comparisons test (E and H).

CXCR6, but not CXCR3, is required for the continual recruitment of cells from the lung interstitium to the airways

We next sought to determine the factors regulating the continual migration of lung interstitium-resident memory CD8⁺ T cells to the airways. Among several chemokine receptors examined, CXCR3 and CXCR6 were found to be highly expressed on the surface of memory CD8⁺ T cells in the lung interstitium (Fig. 4 A). Using a parabiosis approach (as described in Fig. 1 A using reporter mice carrying GFP knocked into one allele of the *Cxcr6* locus), we demonstrated that while CXCR3 was expressed on both host and partner memory CD8⁺ T cells in the lung interstitium, high expression of CXCR6 was unique to host cells, especially CD69⁺ T_{RM} cells, where cells are being reactivated (Fig. 4 B). Chemotaxis studies were consistent with this pattern of chemokine receptor expression. While host and partner memory CD8⁺ T cells showed similar levels of chemotaxis to CXCL10, a ligand of CXCR3, chemotaxis to CXCL16, a ligand of CXCR6, was exclusive in host CD8⁺ T_{RM} cells but not partner-derived T_{EM} cells in the lung interstitium (Fig. 4 C). These observations suggest the potential role of the CXCR6–CXCL16 axis in the continual migration of cells from the lung interstitium to the epithelium.

Although the expression of CXCL16 is strongly enhanced in response to inflammatory stimuli and leads to recruitment of activated T cells into inflamed tissues (Matloubian et al., 2000; Abel et al., 2004; Gough et al., 2004), constitutive expression of CXCL16 has also been reported in a variety of resting tissues, including the lung (van der Voort et al., 2010). Thus, we sought to identify CXCL16-producing cells in situ. As shown in Fig. 4 D, strong expression of CXCL16 protein was observed in a majority of epithelial cells, including those surrounding the lymphocytic infiltration in the lung of flu-immune memory mice. Furthermore, real-time PCR analysis revealed that it is epithelial cells (EpCAM⁺) and alveolar macrophages (Siglec F⁺) that highly expressed *Cxcl16* mRNA under steady-state conditions (Fig. 4 E, see not infected and day 30 after infection), despite the lower expression levels relative to the early phase of infection (Fig. 4 E, see day 5 after infection). These findings strongly suggest the involvement of CXCL16 in steady-state recruitment of lung interstitium CD8⁺ T_{RM} cells to the airway epithelium, and prompted us to demonstrate whether intraepithelial migration could be inhibited by administration of neutralizing Ab against this chemokine (Fig. 4 F). As expected, blockade of CXCL16–CXCR6 interaction significantly inhibited the intraepithelial migration of host CD8⁺ T_{RM} cells (as determined by loss of CD11a⁺ cells in the lung airways), whereas the migratory property of partner cells was not affected (Fig. 4 G). The data thus far demonstrated that CXCL16 produced by lung epithelial cells and alveolar macrophages is a major driving force that regulates continual recruitment of lung interstitium CD8⁺ T_{RM} cells into the epithelium. Interestingly, when we blocked chemokine

receptor CXCR3 in the parabiosis experiments, we also observed significant reduction in ratio of partner cells in the lung airways (Fig. 4 H), suggesting that CXCR3 plays a key role in the intraepithelial migration of CD8⁺ T_{EM} cells. Although CXCR3 ligands are known to be expressed in the lung transiently during the acute phase of respiratory virus infection (Wareing et al., 2004; Kohlmeier et al., 2008), we detected steady-state expression of *Cxcl9* mRNA (the expression of which is largely dependent on IFN- γ -mediated upstream signaling; Bachelier et al., 2014) in a variety of cells in the lung including epithelial cells and alveolar macrophages as compared with corresponding cells purified from IFN- γ KO naive mice as a control (Fig. 4 E). These observations suggest that basal levels of CXCR3 ligands expression continued even under steady-state condition, presumably due to continuous exposure to airborne contaminants, which facilitates basal recruitment of tissue-circulating CD8⁺ T_{EM} cells to the airways. Taken together, although steady-state intraepithelial migration of CD8⁺ T_{EM} cells depends on CXCR3, CXCR6 is a major factor that regulates continual recruitment of CD8⁺ T_{RM} cells to the airways (Fig. 5).

Our data address the ongoing debate regarding the maintenance of CD8⁺ T_{RM} cells in the lung by providing definitive evidence that CD8⁺ T_{RM} cells and CD8⁺ T_{EM} cells are maintained by distinct mechanisms. While maintenance of CD8⁺ T_{EM} cells is likely regulated outside the lung tissues, CD8⁺ T_{RM} cells undergo tissue-specific homeostatic proliferation in the lung interstitium, presumably within repair-associated memory depots (RAMD; Takamura et al., 2016), and continuously seed memory to the front-line tissue using a unique chemokine receptor CXCR6 (Fig. 5). We are aware that some CD8⁺ T_{EM} cells may transit through the lung tissues into the airways in response to basal levels of CXCR3 ligands (Fig. 5). Although we do not absolutely exclude the possibility that some tissue-circulating CD8⁺ T_{EM} cells convert into T_{RM} cells (Slütter et al., 2017) as a small fraction of partner cells in the lung interstitium express CD69 and CD103 (Fig. 1 B; Takamura and Kohlmeier, 2019), their contribution to the maintenance of T_{RM} cells is minimal, as demonstrated by our long-term parabiosis experiments. Hence, in contrast to the dynamic nature of airway memory, CD8⁺ T_{RM} cells in the lung interstitium are a stable population that was maintained almost exclusively independently of T_{EM} cells. This conflicts with a previous evidence (Slütter et al., 2017), and the difference is likely due to the fact that Slütter et al. (2017) did not use a parabiosis approach and also did not separate cells in the lung interstitium and airways, thereby including all lung cell populations (e.g., T_{RM}, T_{EM}, and a dynamic population of airway memory cells) in their analysis of T_{RM} cells in the lung interstitium. Furthermore, our finding that different chemokine receptors regulate the intraepithelial migration of T_{RM} and T_{EM} cells resolves another contradiction. A lack of CXCR3 has minimum impact on the maintenance (continual recruitment) of

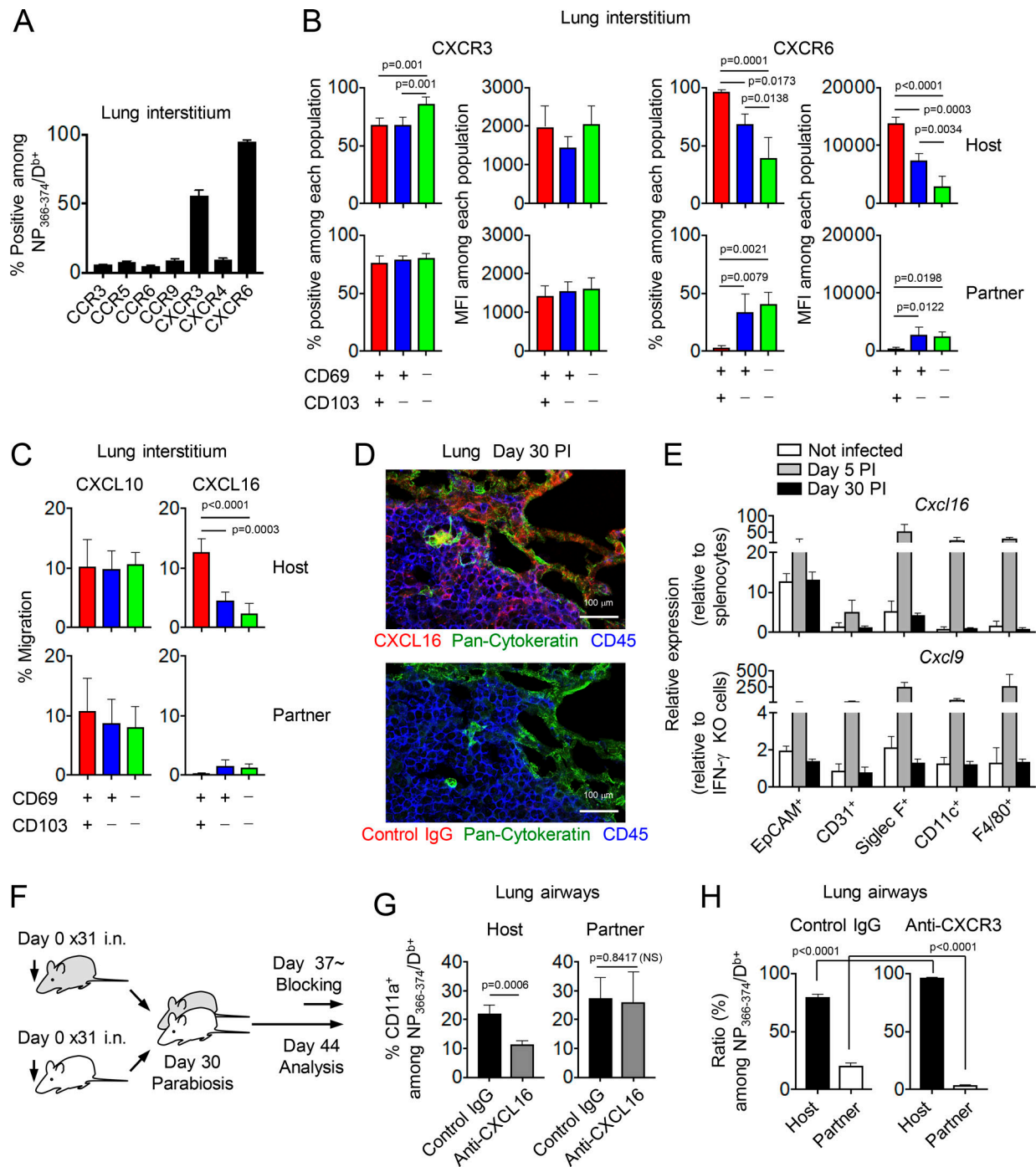


Figure 4. Distinct chemokine receptor usage by T_{RM} and T_{EM} cells upon steady-state migration to the lung airways. (A) Expression of chemokine receptors on NP-specific $CD8^+$ T cells in the lung interstitium of mice on day 30 after x31 infection (i.n.). **(B)** Frequencies of chemokine receptor-expressing cells and intensities of chemokine receptor expression on indicated populations of host and partner NP-specific $CD8^+$ T cells in the lung interstitium at day 14 after surgery. **(C)** CXCL10- and CXCL16-specific chemotaxis of host and partner NP-specific $CD8^+$ T cells in the lung interstitium. **(D)** Immunofluorescence of CXCL16 in lung tissues of mice on day 30 after x31 infection (i.n.). Pan-cytokeratin, green; CXCL16 or isotype control, red; CD45, blue. Scale bars, 100 μ m. **(E)** Expression of indicated mRNAs isolated from each cell fraction in the lung at indicated time points (see Fig. S1). **(F)** Experimental design for G and H. Congenic mice were infected i.n. with x31 and subjected to parabiotic surgery 30 d later. Pairs of mice were treated i.n. with either anti-CXCL16 neutralization Ab or CXCR3 blockade Ab from day 37 after infection. Abs were administered every other day for 1 wk. **(G)** Ratios of $CD11a^+$ cells among host and partner NP-specific $CD8^+$ T cells in the lung airways after Ab treatment. **(H)** Host/partner ratios of NP-specific $CD8^+$ T cells in the lung airways after Ab treatment. Data are representative of two independent experiments (mean and SD of four [B–D and F–H] to five [A and E] mice per group). Error bars represent mean \pm SD of four (B–D and F–H) or five (A and E) mice per group. Data were analyzed by one-way ANOVA with Tukey’s multiple comparisons test (B and C), and unpaired t test (G and H). MFI, mean fluorescent intensity; PI, post-infection.

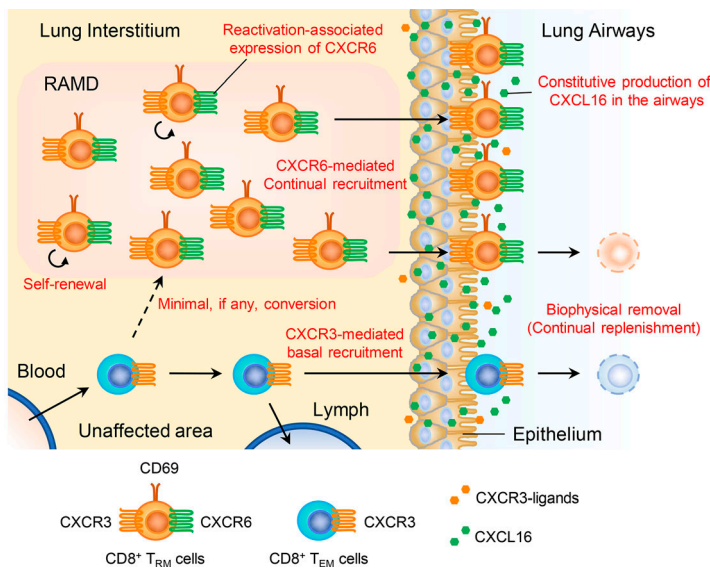


Figure 5. Schematic model of the maintenance of CD8⁺ T_{RM} and T_{EM} cells in the lung. In the lung interstitium, CD8⁺ T_{RM} cells (a major population) are predominantly localized in the RAMD, while CD8⁺ T_{EM} cells (a minor population) distribute sparsely in unaffected areas. Re-activation of CD8⁺ T_{RM} cells leads to up-regulation of CXCR6, which drives continual migration to the airway in response to CXCL16 expressed constitutively in the lung airways. Some CD8⁺ T_{RM} cells in the RAMD undergo homeostatic proliferation to compensate for the continuous loss of cells by intraepithelial migration. Lung interstitium CD8⁺ T_{RM} cells are primarily maintained independently of CD8⁺ T_{EM} cells, although a low level of T_{EM} to T_{RM} cell conversion may occur. While tissue-circulating CD8⁺ T_{EM} cells in the lung interstitium leave tissues via lymphatics, some cells migrate to the airways in response to CXCR3 ligands. Airway memory CD8⁺ T cells are continuously replenished by new cells recruited from the lung interstitium. Red text indicates new findings from our current study.

airway CD8⁺ T_{RM} cells generated by respiratory virus infection (Kohlmeier et al., 2011). However, defective steady-state recruitment of memory CD8⁺ T cells to the lung airways in the absence of CXCR3 was evident in a model of systemic infection (Slütter et al., 2013). This is likely because respiratory virus infection elicits bona fide T_{RM} cells in the lung interstitium that can use CXCR6 in their migration to the airways (CXCR3-independent migration), whereas systemic infection elicits mainly T_{EM} but not T_{RM} cells in the lung, so their airway migration relies mostly on CXCR3. Thus, in addition to the previous findings regarding the limited lifespan of airway memory (Ely et al., 2006), most published data in the field fit with our model of continual recruitment of airway memory cells from T_{RM} cells in the interstitium.

Despite considerable progress in understanding the mechanisms by which CD8⁺ T_{RM} cells are maintained in the lung, we still do not understand the mechanisms responsible for the more rapid waning of lung CD8⁺ T_{RM} cells, compared to T_{RM} cells in other tissues (Wu et al., 2014; Slütter et al., 2017). It seems likely that the lower turnover rate of tissue memory T cells and the loss of lung T_{RM} cell niches (RAMD) as a result of tissue repair probably contribute to their short-lived nature (Takamura et al., 2016; Takamura, 2017). Furthermore, time-dependent loss of T_{EM} cells in the circulation may also contribute (Slütter et al., 2017). Gradual decline of both T_{RM} and T_{EM} cell populations over the course of infection may explain the relatively stable ratio of host and partner cells (without skewing to either population) in the long-term parabiosis experiments. Given the relationship between CXCR6 expression and re-activation of T_{RM} cells, a full understanding of the mechanisms of T_{RM} cell reactivation in the lung interstitium as well as tissue-driven homeostatic proliferation are the key for future research targets to extend the longevity of front-line memory in the lung.

Materials and methods

Mice, virus, and infections

Influenza viruses x31 and x31-OVA₁ expressing the SIINFEKL epitope (provided by the Trudeau Institute, Saranac Lake, NY

with the permission of E. Hoffmann and R. Webby, St. Jude Children's Research Hospital, Memphis, TN) were grown, stored, and titered as described (Takamura et al., 2016). B6 mice were purchased from CLEA Japan. B6.PL-*Thy1^a*/CyJ mice (CD90.1⁺), B6.SJL-*Ptprc^a* *Pepc^b*/BoyJ mice (CD45.1⁺), and B6.129P2-*Cxcr6^{tmLitt}*/J mice were purchased from the Jackson Laboratory. C57BL/6-Tg(*TcrαTcrβ*)1100Mjb/J (OT-1) mice were provided by M. Azuma (Tokyo Medical and Dental University, Tokyo, Japan) with the permission of W.R. Heath (University of Melbourne, Melbourne, Australia). Fucci Tg mice (B6 background) that express monomeric Kusabira-Orange 2-tagged Geminin and monomeric Azami-Green-tagged Cdt1 (Sakaue-Sawano et al., 2008) were provided by M. Tomura. IFN-γ KO mice (B6 background) were provided by Y. Iwakura (Tokyo University of Science, Tokyo, Japan; Tagawa et al., 1997). Mice (6–10 wk) were infected i.n. (300 egg infectious dose [EID₅₀]) or i.p. (10⁴ EID₅₀) with x31. All animal studies were approved by Kindai University.

Parabiosis and Ab treatments

Mice were anesthetized and flank hair removed with a clipper. A longitudinal skin incision was made from the knee to the elbow on a single lateral side along with a 5-mm lateral peritoneal incision. Two mice were joined together by suturing each reciprocal peritoneal opening. Two mattress stiches were made on the lateral edges of the skin section to hold the mice in the upright position, and the dorsal and ventral sides of the skin section of each mouse were further joined with wound clips. Blood was obtained from mice at 10 d after the surgery to confirm equilibration. In some studies, pairs of mice were injected i.n. with 30 μg of Anti-SR-PSOX/CXCL16 Ab (Fukumoto et al., 2004), or 30 μg of anti-CXCR3 Ab clone CXCR3-173 (Bio X Cell). Abs were administered every other day for 1 wk.

OT-1 cell transfer

Splenocytes from male OT-1 mice were enriched for CD8⁺ cells by negative selection (BD IMag) and stained with anti-CD44-FITC,

and CD44^{lo} cells were isolated using a FACSria cell sorter with DIVA enhancement software (BD Bioscience). A total of 5×10^4 cells were transferred into male or female recipient mice, followed by i.n. infection with x31-OVA₁.

Intratracheal transfer

Total CD8 T cells were enriched from the spleens of C57BL/6 mice at >30 d after x31 infection. Donor cells were labeled with CFSE (Life Technologies) by incubation in PBS containing 0.5–0.7 μ M CSFE for 10 min in the dark. The cells were then washed and resuspended in PBS at a concentration of 2×10^7 cells/ml before transfer. CD45.1⁺ recipient mice were anesthetized, and 50 μ l (10^6 cells) of the cell suspension or PBS was instilled into the lungs (via the trachea) using a 1-ml syringe fitted with a blunted 20-gauge needle.

Tissue harvest and flow cytometry

Mice were injected i.v. with 1 μ g anti-CD8 β 3 min before tissue harvest. Cells in the lung airways were recovered by lavage with PBS (5×1 ml), followed by plastic adherence (1 h at 37°C). Lung tissues were digested by collagenase D (Roche Diagnostics) for 30 min at 37°C, and enriched by centrifugation over a 40/80% Percoll gradient. Spleen cells were obtained by straining through nylon mesh and enriched by panning on anti-mouse IgG-coated flasks, followed by RBC lysis in buffered ammonium chloride. Cells were blocked first with mAbs to Fc γ III/II and then stained with APC-conjugated influenza NP₃₆₆₋₃₇₄/D^b tetramer. MHC class I tetramers were generated by the Molecular Biology Core Facility at the Trudeau Institute as described previously (Takamura et al., 2010). Tetramer-labeled cells were washed and stained with fluorescent-conjugated reagents purchased from BD Bioscience (CD45.1, CD90.1, Siglec F, and CD31), BioLegend (CD8 α , CD8 β , CD44, CD69, CD49a, CD103, CD11a, EpCAM, CCR3, CCR5, CCR6, and CCR9), TONBO Bioscience (CD90.2, CD11c, and F4/80), or R&D Systems (CXCR3, CXCR4, and CXCR6). Samples were run on LSRFortessa flow cytometers (BD Bioscience), and data were analyzed using FlowJo (Tree Star).

BrdU

After parabiotic surgery, pairs of mice were administered BrdU by drinking water (0.8 mg/ml) for 1 wk before harvest. Alternatively, parabiotic mice were administered i.v. with BrdU (2 mg/ml) or CFSE (0.5 mM) at 24, 12, 6, or 1 h before harvest. Single-cell suspensions were stained with tetramers and Abs to surface proteins as described above, and BrdU incorporation was detected using the BrdU Flow Kit (BD Biosciences).

TCR clonotyping

30 d after x31 infection, CD8⁺ NP₃₆₆₋₃₇₄/D^b tetramer⁺ cells in the spleen (~15,000 cells), and CD8⁺CD69⁺NP₃₆₆₋₃₇₄/D^b tetramer⁺ cells in the lung interstitium and airways (~3,000–5,000 cells) were sorted by FACSria II. Unbiased amplification of all expressed TCR β -chain gene products was conducted using a template-switch anchored RT-PCR with a 3' constant region primer (5'-TGGCTCAAACAAGGAGACCT-3'). Amplicons were subcloned, sampled, sequenced, and analyzed

as described previously (Quigley et al., 2011). The ImMunoGeneTics database (<http://www.imgt.org/>) was used to assign TRB gene usage. Detailed TCR β chain profiles are shown in Dataset 1.

Chemotaxis assay

Migration of CD8⁺ T cells of x31-infected mice was analyzed in Transwell chambers with 5- μ m pore size polycarbonate filters (Corning Life Sciences). 10^6 cells were added to the upper chamber. An optimal concentration of either extracellular domain of recombinant CXCL16 (500 μ g/ml; R&D Systems) or recombinant murine CXCL10 (10^{-8} M; Peprotech) was prepared in the serum-free medium (Hybridoma-SFM Complete DPM; Gibco) and added to the lower chamber. After incubation at 37°C in 5% CO₂ for 4 h, the number of cells in the upper and lower chambers was analyzed by flow cytometry. Percent migration was calculated as $(n \text{ cells in the lower chamber}) / [(n \text{ cells in the upper chamber}) + (n \text{ cells in the lower chamber})] \times 100$.

Real-time PCR

Before and after x31 infection, each fraction of cells shown in Fig. S1 was sorted on a FACSria (BD Bioscience). Total RNA was prepared using the RNeasy Plus Mini Kit (Qiagen), and cDNA synthesis was performed by using the PrimeScript RT Reagent Kit (TaKaRa). Quantitative PCR (qPCR) was performed using a StepOnePlus Real-Time PCR system (ABI) in a 96-well plate format with SYBR Green-based detection (TaKaRa). β -actin mRNA was used for normalization. Primers used were *Cxcl6* forward, 5'-GGCTTTGGACCCTTGCTCTTG-3', *Cxcl6* reverse, 5'-TTGCGCTCAAAGCAGTCCACT-3'; *Cxcl9* forward, 5'-TGTGGA GTTCGAGGAACCT-3', and *CXCL9* reverse, 5'-TGCCTTGCTGG TGCTG-3'. mRNA levels in the splenocytes of uninfected animals (for *Cxcl6*) and corresponding cells purified from IFN- γ KO mice (for *Cxcl9*) were used as a standard, and relative expression of mRNA was calculated as $2^{-\Delta\text{Ct}}$.

Immunofluorescence

At day 30 after x31 infection, lung tissues were harvested, embedded in OCT compound (Sakura Finetek), and frozen in liquid nitrogen. 6- μ m-thick cryosections were prepared and fixed for 10 min with acetone. Fixed sections were rehydrated with PBS, blocked with Blocking One reagent (Nacalai Tesque), and stained with a mixture of Abs against CD45 (30-F11; BD Biosciences), Pan-Cytokeratin (rabbit polyclonal; Bioss), and either CXCL16 (goat polyclonal; R&D Systems) or control Abs (goat IgG; Jackson Immunoresearch) dissolved in PBS containing 2% BSA for 30 min at 37°C. Sections were further incubated with Alexa Fluor-labeled appropriate secondary Abs. After the staining, sections were mounted with Prolong Gold reagent (Life Technologies) and then photographed using an SP5 confocal microscope (Leica Microsystems).

Statistical analysis

Statistical analysis was performed with Prism software (GraphPad). Methods of comparison and corrections for multiple comparisons are indicated in each relevant figure legend.

Online supplemental material

Fig. S1 shows a gating strategy for the isolation of each cell population in the lung for qPCR analysis, which is related to Fig. 4 E. Dataset 1 shows TCR β chain profiles of NP-specific CD8⁺ T cells in each tissue, which is related to Fig. 2.

Acknowledgments

We thank the Center for Instrumental Analysis, Central Research Facilities, Kindai University Faculty of Medicine (CRF), for assistance with flow cytometry, the Center for Animal Experiments, CRF, for animal care, the Center for Recombinant DNA Experiments, CRF, for infection experiments, the Center of Morphological Analysis, CRF, for histology, William Reiley (Trudeau Institute, Saranac Lake, NY) for tetramers, members of the Miyazawa laboratory for discussions, and David L. Woodland for assistance in editing the manuscript.

This work was supported by the Ministry of Education, Culture, Sports, Science and Technology of Japan with a Grant-in-Aid for Young Scientists (A) 24689043 (S. Takamura) and for Scientific Research on Innovative Areas 15H01268 (M. Miyazawa). This work was also supported by grants from the Takeda Science Foundation (S. Takamura), Daiichi-Sankyo Foundation of Life Science (S. Takamura), Uehara Memorial Foundation (S. Takamura), Kanae Foundation for the Promotion of Medical Science (S. Takamura), and Kindai University Anti-Aging Center (M. Miyazawa).

The authors declare no competing financial interests.

Author contributions: Conceptualization, S. Takamura; Methodology, S. Takamura; Validation, S. Takamura; Formal analysis, S. Takamura, S. Kato, and C. Motozono; Investigation, S. Takamura, S. Kato, C. Motozono, T. Shimaoka, S. Ueha, T. Masumoto, and A. Katsushima; Resources, T. Shimaoka, K. Matsuo, K. Miyauchi, T. Nakayama, M. Tomura, K. Matsushima, M. Kubo, and M. Miyazawa; Writing—original draft, S. Takamura; Writing—review and editing, S. Takamura; Visualization, S. Takamura; Supervision, S. Takamura; Project administration, S. Takamura; and Funding acquisition, S. Takamura.

Submitted: 27 March 2019

Revised: 10 July 2019

Accepted: 4 September 2019

References

Abel, S., C. Hundhausen, R. Mentlein, A. Schulte, T.A. Berkhout, N. Broadway, D. Hartmann, R. Sedlacek, S. Dietrich, B. Muetze, et al. 2004. The transmembrane CXC-chemokine ligand 16 is induced by IFN- γ and TNF- α and shed by the activity of the disintegrin-like metalloproteinase ADAM10. *J. Immunol.* 172:6362–6372. <https://doi.org/10.4049/jimmunol.172.10.6362>

Bachelier, F., A. Ben-Baruch, A.M. Burkhardt, C. Combadiere, J.M. Farber, G.J. Graham, R. Horuk, A.H. Sparre-Ulrich, M. Locati, A.D. Luster, et al. 2014. International Union of Basic and Clinical Pharmacology. [corrected]. LXXXIX. Update on the extended family of chemokine receptors and introducing a new nomenclature for atypical chemokine receptors. *Pharmacol. Rev.* 66:1–79. <https://doi.org/10.1124/pr.113.007724>

Ely, K.H., T. Cookenham, A.D. Roberts, and D.L. Woodland. 2006. Memory T cell populations in the lung airways are maintained by continual

recruitment. *J. Immunol.* 176:537–543. <https://doi.org/10.4049/jimmunol.176.1.537>

Fukumoto, N., T. Shimaoka, H. Fujimura, S. Sakoda, M. Tanaka, T. Kita, and S. Yonehara. 2004. Critical roles of CXC chemokine ligand 16/scavenger receptor that binds phosphatidylserine and oxidized lipoprotein in the pathogenesis of both acute and adoptive transfer experimental autoimmune encephalomyelitis. *J. Immunol.* 173:1620–1627. <https://doi.org/10.4049/jimmunol.173.3.1620>

Gaide, O., R.O. Emerson, X. Jiang, N. Gulati, S. Nizza, C. Desmarais, H. Robins, J.G. Krueger, R.A. Clark, and T.S. Kupper. 2015. Common clonal origin of central and resident memory T cells following skin immunization. *Nat. Med.* 21:647–653. <https://doi.org/10.1038/nm.3860>

Gebhardt, T., P.G. Whitney, A. Zaid, L.K. Mackay, A.G. Brooks, W.R. Heath, F.R. Carbone, and S.N. Mueller. 2011. Different patterns of peripheral migration by memory CD4⁺ and CD8⁺ T cells. *Nature.* 477:216–219. <https://doi.org/10.1038/nature10339>

Gerlach, C., E.A. Moseman, S.M. Loughhead, D. Alvarez, A.J. Zwijnenburg, L. Waanders, R. Garg, J.C. de la Torre, and U.H. von Andrian. 2016. The Chemokine Receptor CX3CR1 Defines Three Antigen-Experienced CD8 T Cell Subsets with Distinct Roles in Immune Surveillance and Homeostasis. *Immunity.* 45:1270–1284. <https://doi.org/10.1016/j.immuni.2016.10.018>

Gough, P.J., K.J. Garton, P.T. Wille, M. Rychlewski, P.J. Dempsey, and E.W. Raines. 2004. A disintegrin and metalloproteinase 10-mediated cleavage and shedding regulates the cell surface expression of CXC chemokine ligand 16. *J. Immunol.* 172:3678–3685. <https://doi.org/10.4049/jimmunol.172.6.3678>

Herndler-Brandstetter, D., H. Ishigame, R. Shinnakasu, V. Plajer, C. Stecher, J. Zhao, M. Lietzenmayer, L. Kroehling, A. Takumi, K. Komatani, et al. 2018. KLRG1(+) Effector CD8(+) T Cells Lose KLRG1, Differentiate into All Memory T Cell Lineages, and Convey Enhanced Protective Immunity. *Immunity.* 48:716–729.e8. <https://doi.org/10.1016/j.immuni.2018.03.015>

Hogan, R.J., E.J. Usherwood, W. Zhong, A.A. Roberts, R.W. Dutton, A.G. Harmsen, and D.L. Woodland. 2001. Activated antigen-specific CD8⁺ T cells persist in the lungs following recovery from respiratory virus infections. *J. Immunol.* 166:1813–1822. <https://doi.org/10.4049/jimmunol.166.3.1813>

Hogan, R.J., L.S. Cauley, K.H. Ely, T. Cookenham, A.D. Roberts, J.W. Brennan, S. Monard, and D.L. Woodland. 2002. Long-term maintenance of virus-specific effector memory CD8⁺ T cells in the lung airways depends on proliferation. *J. Immunol.* 169:4976–4981. <https://doi.org/10.4049/jimmunol.169.9.4976>

Kohlmeier, J.E., S.C. Miller, and D.L. Woodland. 2007. Cutting edge: Antigen is not required for the activation and maintenance of virus-specific memory CD8⁺ T cells in the lung airways. *J. Immunol.* 178:4721–4725. <https://doi.org/10.4049/jimmunol.178.8.4721>

Kohlmeier, J.E., S.C. Miller, J. Smith, B. Lu, C. Gerard, T. Cookenham, A.D. Roberts, and D.L. Woodland. 2008. The chemokine receptor CCR5 plays a key role in the early memory CD8⁺ T cell response to respiratory virus infections. *Immunity.* 29:101–113. <https://doi.org/10.1016/j.immuni.2008.05.011>

Kohlmeier, J.E., W.W. Reiley, G. Perona-Wright, M.L. Freeman, E.J. Yager, L.M. Connor, E.L. Brincks, T. Cookenham, A.D. Roberts, C.E. Burkum, et al. 2011. Inflammatory chemokine receptors regulate CD8(+) T cell contraction and memory generation following infection. *J. Exp. Med.* 208:1621–1634. <https://doi.org/10.1084/jem.20102110>

Masopust, D., V. Vezys, A.L. Marzo, and L. LeFrançois. 2001. Preferential localization of effector memory cells in nonlymphoid tissue. *Science.* 291:2413–2417. <https://doi.org/10.1126/science.1058867>

Matloubian, M., A. David, S. Engel, J.E. Ryan, and J.G. Cyster. 2000. A transmembrane CXC chemokine is a ligand for HIV-coreceptor Bonzo. *Nat. Immunol.* 1:298–304. <https://doi.org/10.1038/79738>

McMaster, S.R., J.J. Wilson, H. Wang, and J.E. Kohlmeier. 2015. Airway-Resident Memory CD8 T Cells Provide Antigen-Specific Protection against Respiratory Virus Challenge through Rapid IFN- γ Production. *J. Immunol.* 195:203–209. <https://doi.org/10.4049/jimmunol.1402975>

Quigley, M.F., J.R. Almeida, D.A. Price, and D.C. Douek. 2011. Unbiased molecular analysis of T cell receptor expression using template-switch anchored RT-PCR. *Curr. Protoc. Immunol.* Chapter 10: Unit10.33.

Sakaue-Sawano, A., H. Kurokawa, T. Morimura, A. Hanyu, H. Hama, H. Osawa, S. Kashiwagi, K. Fukami, T. Miyata, H. Miyoshi, et al. 2008. Visualizing spatiotemporal dynamics of multicellular cell-cycle progression. *Cell.* 132:487–498. <https://doi.org/10.1016/j.cell.2007.12.033>

- Sallusto, F., D. Lenig, R. Förster, M. Lipp, and A. Lanzavecchia. 1999. Two subsets of memory T lymphocytes with distinct homing potentials and effector functions. *Nature*. 401:708–712. <https://doi.org/10.1038/44385>
- Schenkel, J.M., K.A. Fraser, L.K. Beura, K.E. Pauken, V. Vezy, and D. Masopust. 2014. T cell memory. Resident memory CD8 T cells trigger protective innate and adaptive immune responses. *Science*. 346:98–101. <https://doi.org/10.1126/science.1254536>
- Slütter, B., L.L. Pewe, S.M. Kaech, and J.T. Harty. 2013. Lung airway-surveillance CXCR3(hi) memory CD8(+) T cells are critical for protection against influenza A virus. *Immunity*. 39:939–948. <https://doi.org/10.1016/j.immuni.2013.09.013>
- Slütter, B., N. Van Braeckel-Budimir, G. Abboud, S.M. Varga, S. Salek-Ardakani, and J.T. Harty. 2017. Dynamics of influenza-induced lung-resident memory T cells underlie waning heterosubtypic immunity. *Sci. Immunol.* 2:eaag2031.
- Steinert, E.M., J.M. Schenkel, K.A. Fraser, L.K. Beura, L.S. Manlove, B.Z. Ignyártó, P.J. Southern, and D. Masopust. 2015. Quantifying Memory CD8 T Cells Reveals Regionalization of Immunosurveillance. *Cell*. 161:737–749. <https://doi.org/10.1016/j.cell.2015.03.031>
- Tagawa, Y., K. Sekikawa, and Y. Iwakura. 1997. Suppression of concanavalin A-induced hepatitis in IFN-gamma(-/-) mice, but not in TNF-alpha(-/-) mice: role for IFN-gamma in activating apoptosis of hepatocytes. *J. Immunol.* 159:1418–1428.
- Takamura, S. 2017. Persistence in Temporary Lung Niches: A Survival Strategy of Lung-Resident Memory CD8⁺ T Cells. *Viral Immunol.* 30:438–450. <https://doi.org/10.1089/vim.2017.0016>
- Takamura, S. 2018. Niches for the Long-Term Maintenance of Tissue-Resident Memory T Cells. *Front. Immunol.* 9:1214. <https://doi.org/10.3389/fimmu.2018.01214>
- Takamura, S., and J.E. Kohlmeier. 2019. Establishment and maintenance of conventional and circulation-driven lung-resident memory CD8⁺ T cells following respiratory virus infections. *Front. Immunol.* 10:733. <https://doi.org/10.3389/fimmu.2019.00733>
- Takamura, S., A.D. Roberts, D.M. Jelley-Gibbs, S.T. Wittmer, J.E. Kohlmeier, and D.L. Woodland. 2010. The route of priming influences the ability of respiratory virus-specific memory CD8⁺ T cells to be activated by residual antigen. *J. Exp. Med.* 207:1153–1160. <https://doi.org/10.1084/jem.20090283>
- Takamura, S., H. Yagi, Y. Hakata, C. Motozono, S.R. McMaster, T. Masumoto, M. Fujisawa, T. Chikaishi, J. Komeda, J. Itoh, et al. 2016. Specific niches for lung-resident memory CD8⁺ T cells at the site of tissue regeneration enable CD69-independent maintenance. *J. Exp. Med.* 213:3057–3073. <https://doi.org/10.1084/jem.20160938>
- Tomura, M., A. Sakaue-Sawano, Y. Mori, M. Takase-Utsugi, A. Hata, K. Ohtawa, O. Kanagawa, and A. Miyawaki. 2013. Contrasting quiescent G0 phase with mitotic cell cycling in the mouse immune system. *PLoS One*. 8:e73801. <https://doi.org/10.1371/journal.pone.0073801>
- van der Voort, R., V. Verweij, T.M. de Witte, E. Lasonder, G.J. Adema, and H. Dolstra. 2010. An alternatively spliced CXCL16 isoform expressed by dendritic cells is a secreted chemoattractant for CXCR6⁺ cells. *J. Leukoc. Biol.* 87:1029–1039. <https://doi.org/10.1189/jlb.0709482>
- Wareing, M.D., A.B. Lyon, B. Lu, C. Gerard, and S.R. Sarawar. 2004. Chemokine expression during the development and resolution of a pulmonary leukocyte response to influenza A virus infection in mice. *J. Leukoc. Biol.* 76:886–895. <https://doi.org/10.1189/jlb.1203644>
- Wu, T., Y. Hu, Y.T. Lee, K.R. Bouchard, A. Benechet, K. Khanna, and L.S. Cauley. 2014. Lung-resident memory CD8 T cells (TRM) are indispensable for optimal cross-protection against pulmonary virus infection. *J. Leukoc. Biol.* 95:215–224. <https://doi.org/10.1189/jlb.0313180>
- Zammit, D.J., D.L. Turner, K.D. Klonowski, L. Lefrançois, and L.S. Cauley. 2006. Residual antigen presentation after influenza virus infection affects CD8 T cell activation and migration. *Immunity*. 24:439–449. <https://doi.org/10.1016/j.immuni.2006.01.015>

Supplemental material

Takamura et al., <https://doi.org/10.1084/jem.20190557>

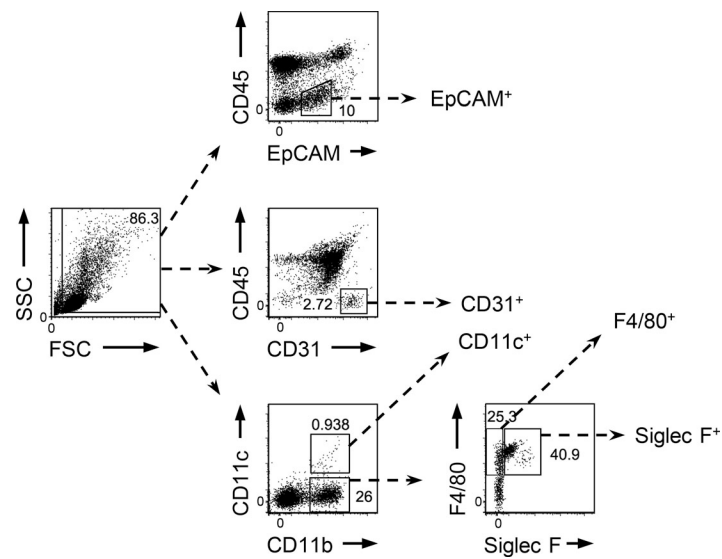


Figure S1. **A gating strategy for the isolation of each cell population in the lung for qPCR analysis.** Related to Fig. 4 E. Example flow-cytometry plots showing the gating strategy for isolation of each cell population in the lung. SSC, side scatter; FSC, forward scatter.

Dataset 1 is provided online as an Excel file and shows TCR β chain profiles of NP-specific CD8⁺ T cells in each tissue, which is related to Fig. 2.